Spatial–temporal patterns at an isolated on-ramp in a new cellular automata model based on three-phase traffic theory

2004 J. Phys. A: Math. Gen. 37 8197

(http://iopscience.iop.org/0305-4470/37/34/001)

INSTITUTE OF PHYSICS PUBLISHING JOURNAL OF PHYSICS A: MATHEMATICAL AND GENERAL

J. Phys. A: Math. Gen. **37** (2004) 8197–8213 PII: S0305-4470(04)81231-9

Spatial–temporal patterns at an isolated on-ramp in a new cellular automata model based on three-phase traffic theory

Rui Jiang and Qing-Song Wu

School of Engineering Science, University of Science and Technology of China, Hefei 230026, People's Republic of China

E-mail: qswu@ustc.edu.cn

Received 24 May 2004
Published 11 August 2004
Online at stacks.iop.org/JPhysA/37/8197
doi:10.1088/0305-4470/37/34/001

Abstract

This paper studies the spatial–temporal patterns at an isolated on-ramp using a new cellular automata model based on three-phase traffic theory. The model may describe the synchronized flow quite satisfactorily (Jiang and Wu 2003 *J. Phys. A: Math. Gen.* **36** 381). The simulations show that six different regions may be classified in the new model induced by an isolated on-ramp. The spacetime plots of the patterns as well as the metastability are investigated. Comparison with the empirical data is made and the qualitative similarity is pointed out. The future work of extension from single-lane simulation to the multi-lane case is pointed out.

PACS numbers: 05.65.+b, 45.70.Vn

1. Introduction

The systematic investigation of traffic flow has quite a long history (see, e.g., [1–9]) and such real traffic phenomena as stop-and-go traffic, capacity drop, phantom jams, hysteresis effects and metastable states are observed. Recently, a more detailed analysis of empirical data has been given by Kerner and his colleague [7–9]. They pointed out that the traffic flow can be either free or congested and the congested flow can be further distinguished into synchronized flow and wide moving jams. The complex spatio-temporal behaviour of real traffic is due to the transitions between the three traffic phases.

Different explanations of these empirical findings and different models have been proposed by various groups in the last few years [1–3]. Most models may be classified into the 'fundamental diagram approach' since the steady-state solutions of these models belong to a

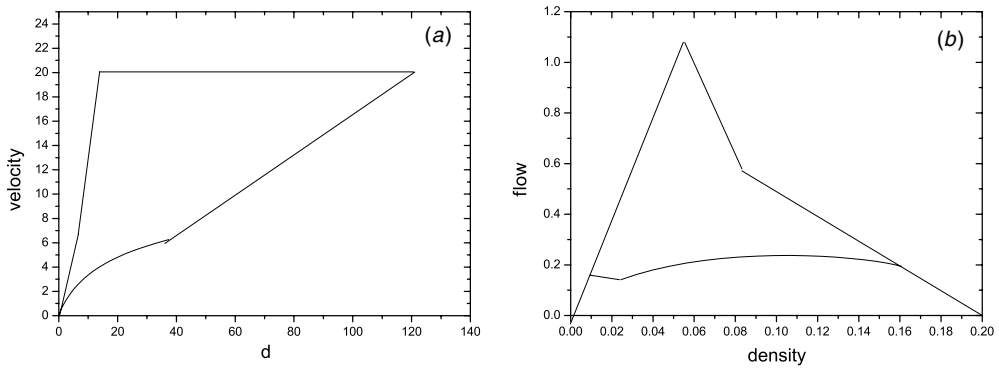

Figure 1. The two-dimensional region of the steady states in the speed–gap plane (*a*) and hence in the flow–density plane (*b*) of the new model in the noiseless limit.

curve in the flow–density plane [10–12]. This curve, which goes through the origin and has at least one maximum, is called the fundamental diagram for traffic flow.

The fundamental diagram approach is successful in explaining several aspects of real traffic such as the forming of queues, the evacuation of jams, etc. However, as pointed out by Kener [13–16], the phase transitions and most of empirical spatial–temporal pattern features are qualitatively different from those which follow from the mathematical traffic flow models in the fundamental diagram approach. For example, empirical observations at an isolated on-ramp showed that (i) a low flow rate to the on-ramp will lead to synchronized flow where the density is relatively low and the speed is relatively high and no moving jams should emerge; (ii) moving jams must spontaneously emerge in synchronized flow upstream of the on-ramp at any high flow rate to the on-ramp. Nevertheless, the simulation results of the fundamental diagram approach are: (i) a low flow rate to the on-ramp leads to different kinds of moving jams such as triggered stop-and-go traffic (TSG) [11] and oscillating congested traffic (OCT) [11]; (ii) homogeneous congested traffic (HCT) [11] where the density is high and the speed is very low occurs when the flow rate to the on-ramp is high and no moving jams spontaneously emerge. This is in contradiction with the observations [11–15].

Kerner introduced a three-phase traffic theory which postulates that the steady states (homogeneous and stationary states, time-independent solutions in which all vehicles move with the same constant speed) of synchronized flow cover a two-dimensional region in the flow–density plane, i.e., there is no fundamental diagram of traffic flow [13–16]. The simulations show that the empirical spatial–temporal pattern features of traffic flow may be reproduced in this theory.

Recently, the authors proposed a new cellular automata model, which can reproduce the synchronized flow quite satisfactorily [17]. The model is based on the comfortable driving (CD) model presented by Knospe *et al* [18], but it meets the fundamental hypothesis of three-phase traffic theory that some steady-state model solutions cover a two-dimensional region in the flow–density plane. In this paper, we study the traffic patterns induced by an isolated on-ramp in the new model and find that the results are consistent with the empirical data.

The paper is organized as follows. In section 2, the new model is briefly reviewed and the satisfaction of the fundamental hypothesis of three-phase traffic theory is provided. The boundary conditions and the on-ramp setup are presented. In section 3, the simulation results are analysed and compared with the empirical data. Conclusions are given in section 4.

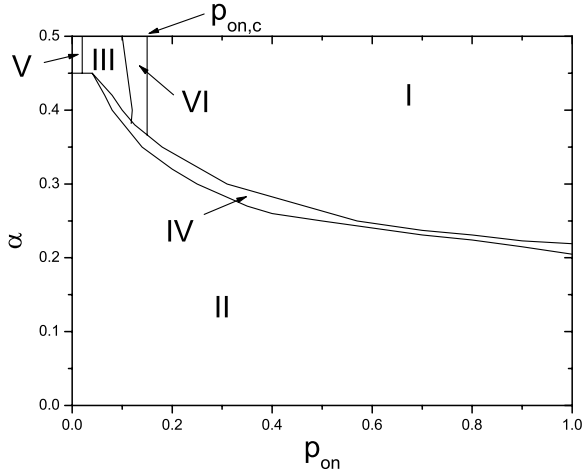

Figure 2. The phase diagram of the new model on an isolated on-ramp.

2. Model, open boundary conditions and on-ramp setup

For the sake of the completeness, we briefly recall the new model. The parallel update rules of the model are as follows:

1. Determination of the randomization parameter $p_n(t+1)$:
   $p_n(t+1) = p(v_n(t), b_{n+1}(t), t_{h,n}, t_{s,n})$.
2. Acceleration:
   if $((b_{n+1}(t) = 0$ or $t_{h,n} \geqslant t_{s,n})$ and $(v_n(t) > 0))$ then
   $v_n(t+1) = \min(v_n(t) + 2, v_{\max})$
   else if $(v_n(t) = 0)$ then
   $v_n(t+1) = \min(v_n(t) + 1, v_{\max})$
   else
   $v_n(t+1) = v_n(t)$.
3. Braking rule:
   $v_n(t+1) = \min\left(d_n^{\text{eff}}, v_n(t+1)\right)$.
4. Randomization and braking:
   if $(\text{rand}() < p_n(t+1))$ then $v_n(t+1) = \max(v_n(t+1) - 1, 0)$.
5. The determination of $b_n(t+1)$:
   if $(v_n(t+1) < v_n(t))$ then $b_n(t+1) = 1$
   if $(v_n(t+1) > v_n(t))$ then $b_n(t+1) = 0$
   if $(v_n(t+1) = v_n(t))$ then $b_n(t+1) = b_n(t)$.
6. The determination of $t_{st,n}$:
   if $v_n(t+1) = 0$ then $t_{st,n} = t_{st,n} + 1$
   if $v_n(t+1) > 0$ then $t_{st,n} = 0$.
7. Car motion:
   $x_n(t+1) = x_n(t) + v_n(t+1)$.

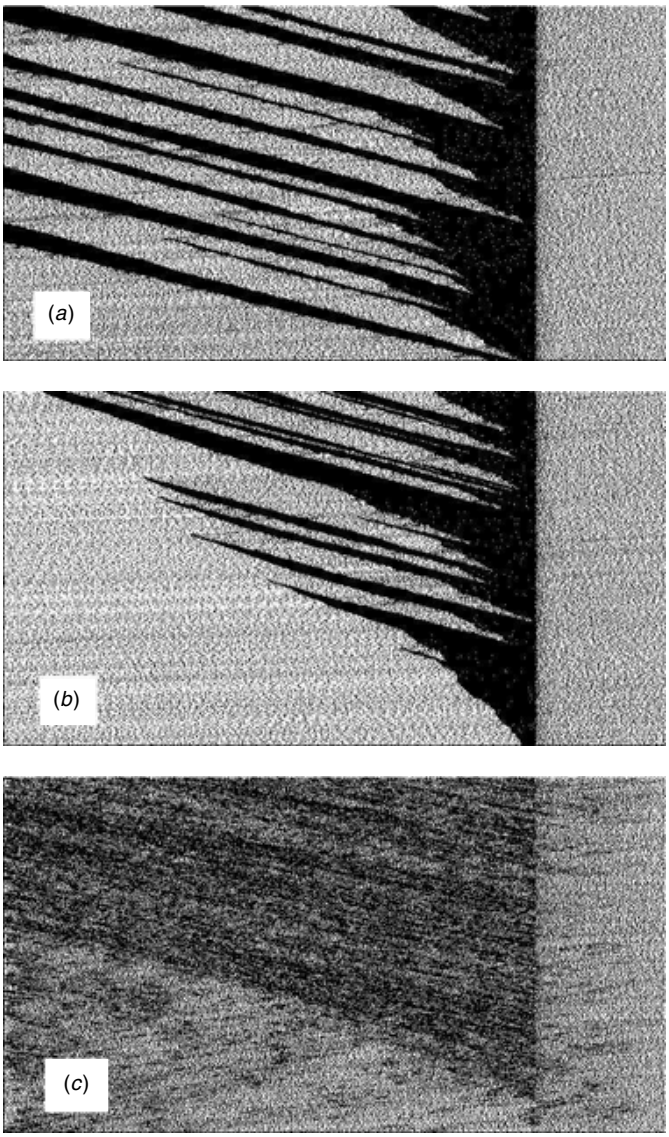

Figure 3. The spacetime plots of the congested patterns. (*a*), (*b*) GP; (*c*) WSP; (*d*), (*e*) LSP; (*f*) ASP; (*g*) DGP. In (*a*) $p_{\rm on} = 0.6, \alpha = 0.4$; (*b*) $p_{\rm on} = 0.8, \alpha = 0.28$; (*c*) $p_{\rm on} = 0.07, \alpha = 0.5$; (*d*) $p_{\rm on} = 0.3, \alpha = 0.3$; (*e*) $p_{\rm on} = 0.28, \alpha = 0.3$; (*f*) $p_{\rm on} = 0.02, \alpha = 0.5$; (*g*) $p_{\rm on} = 0.12, \alpha = 0.5$. The cars are moving from the left to the right, and the vertical direction (up) is (increasing) time. The vertical direction corresponds to 10 000 time steps in (*a*)–(*e*), 3000 time steps in (*f*), 7000 time steps in (*g*). The time intervals are 10 time steps and the trace of every two vehicles is plotted.

Here x_n and v_n are the position and velocity of vehicle n (here vehicle $n+1$ precedes vehicle n), d_n is the gap of the vehicle n, b_n is the status of the brake light (on(off) $\rightarrow$ $b_n = 1(0)$). The two times $t_{h,n} = d_n/v_n(t)$ and $t_{s,n} = \min(v_n(t), h)$, where h determines the range of interaction with the brake light, are introduced to compare the time $t_{h,n}$ needed to

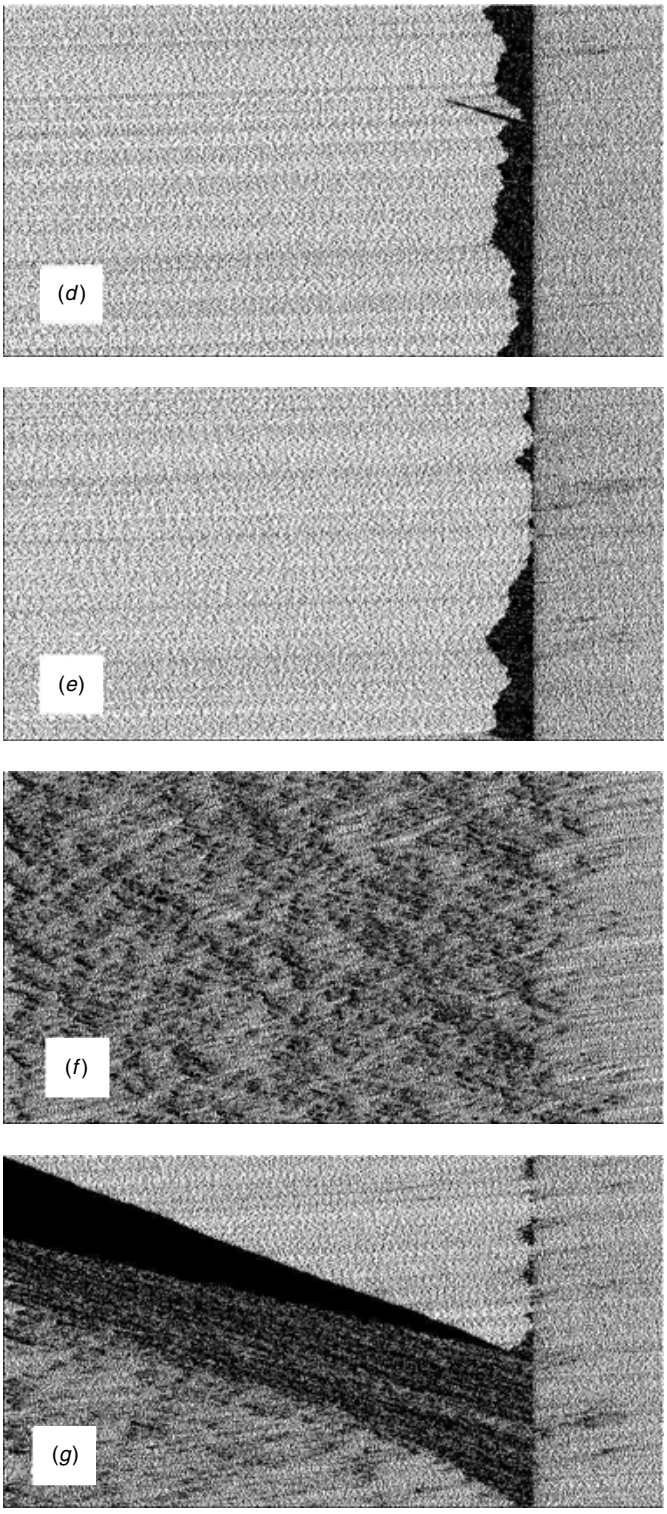

Figure 3. (Continued.)

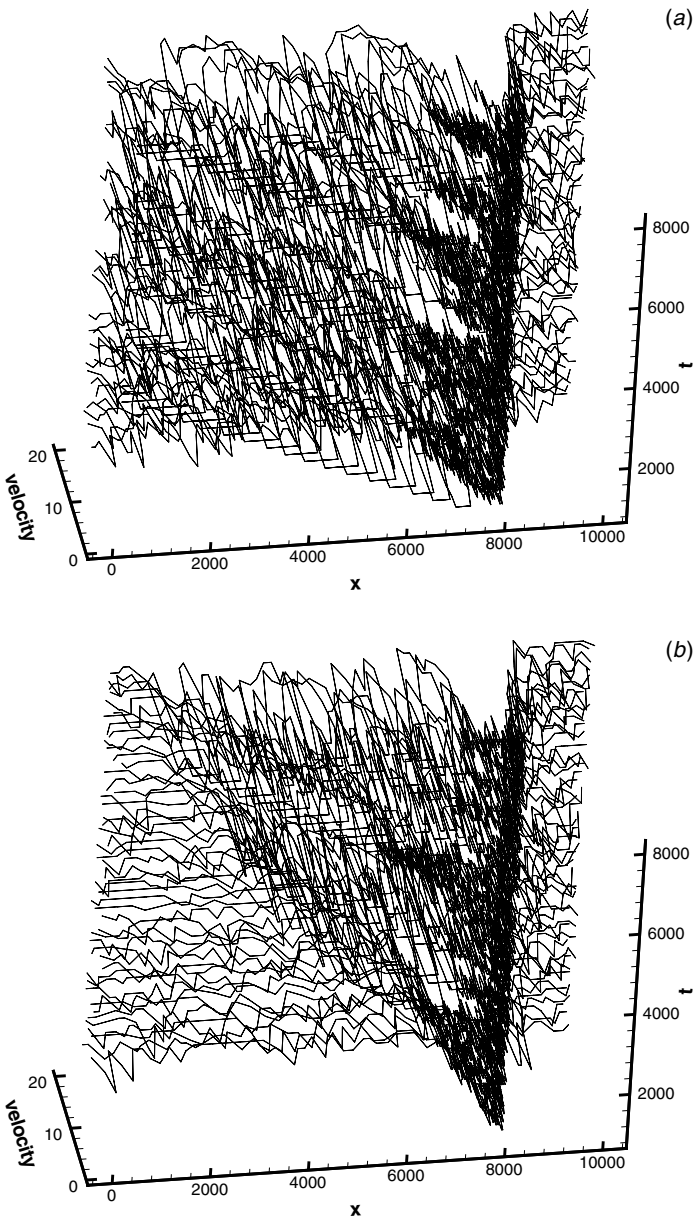

Figure 4. The 3D velocity plots of the congested patterns corresponding to figure 3. The dense region corresponds to synchronized flow, the dilute region to free flow and the jam is characterized by very low speed.

reach the position of the leading vehicle with a velocity-dependent interaction horizon $t_{s,n}$. $d_n^{\text{eff}} = d_n + \max(v_{\text{anti}} - \text{gap}_{\text{safety}}, 0)$ is the effective distance, where $v_{\text{anti}} = \min(d_{n+1}, v_{n+1})$ is the expected velocity of the preceding vehicle in the next time step and $\text{gap}_{\text{safety}}$ controls the effectiveness of the anticipation. rand() is a random number between 0 and 1, $t_{st,n}$ denotes the

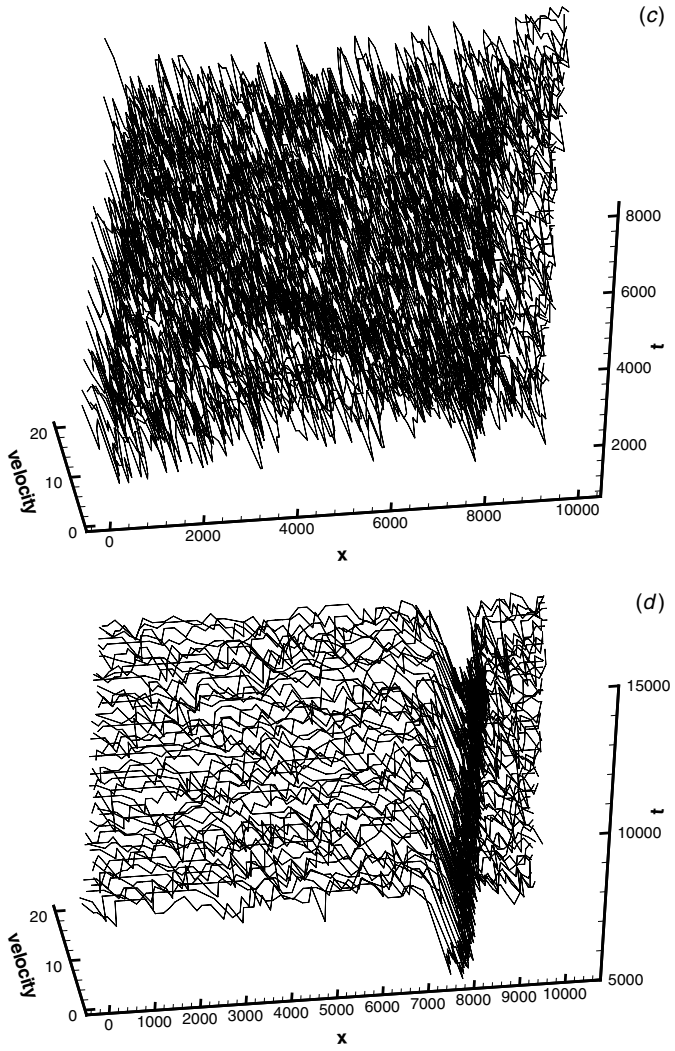

Figure 4. (Continued.)

time that the car n stops. The randomization parameter p is defined:

$$p(v_n(t), b_{n+1}(t), t_{h,n}, t_{s,n}) = \begin{cases} p_b & \text{if} \quad \mathrm{b}_{n+1} = 1 \quad \text{and} \quad t_{h,n} < t_{s,n} \\ p_0 & \text{if} \quad v_n = 0 \quad \text{and} \quad t_{st,n} \geqslant t_c \\ p_d & \text{in all other cases.} \end{cases}$$

Here t_c is a parameter.

As shown later, the new model can reproduce the empirical features at the on-ramp while the CD model cannot. The improvement of the new model over the CD model mainly lies in that the brake light rule is changed. Moreover, the acceleration rule also contributes to the improvement.

In what follows, we show the steady states of the model cover a two-dimensional region in the flow–density plane in the noiseless limit. In the steady state, the velocity of a vehicle

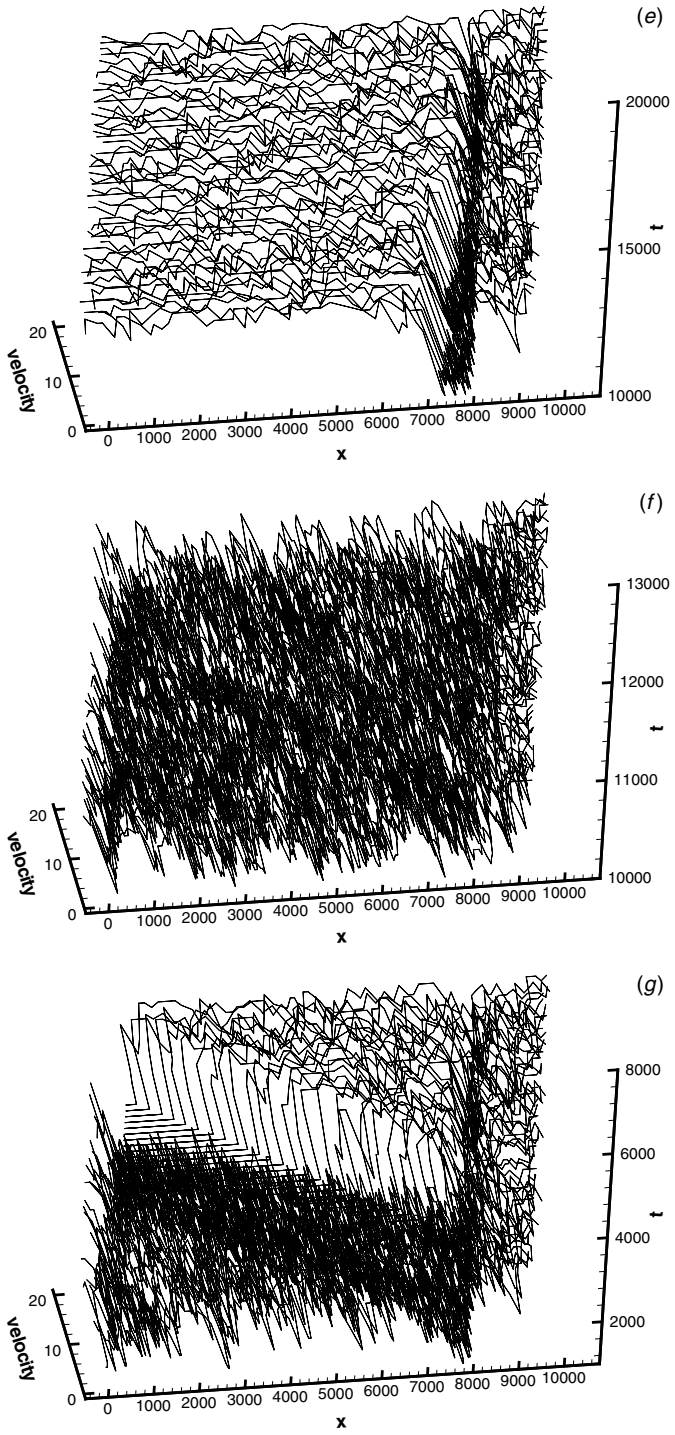

Figure 4. (Continued.)

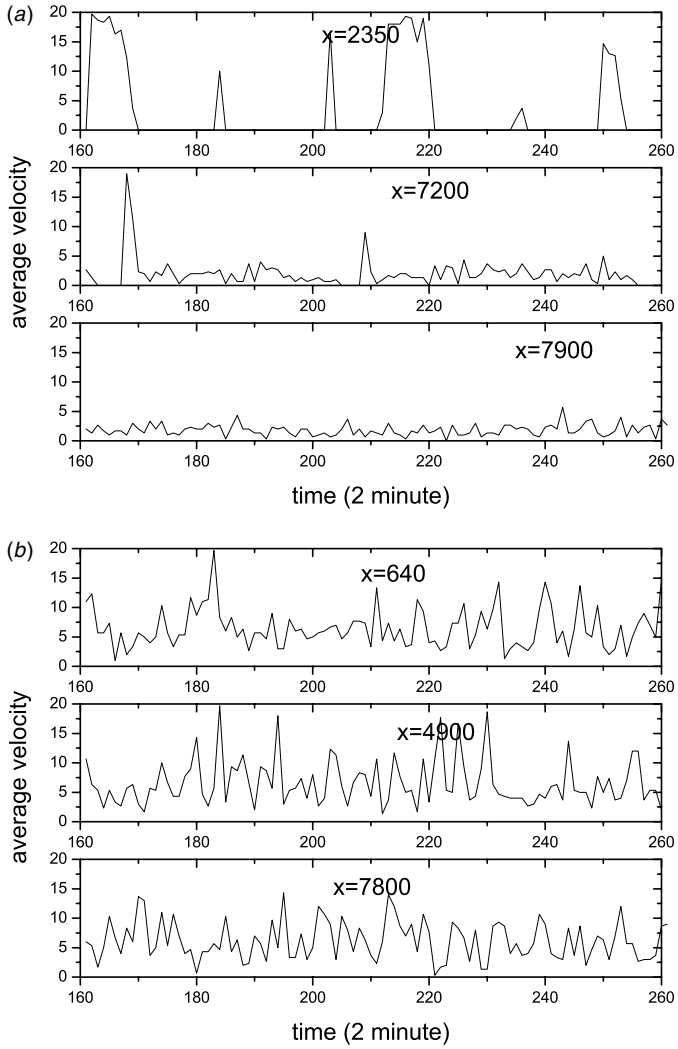

Figure 5. The average velocity observed at a fixed location. (*a*) Corresponds to figure 3(*a*); (*b*) to figure 3(*c*); (*c*) to figure 3(*d*); (*d*) to figure 3(*f*). In (*d*), the circles indicate the average velocity in free flow.

remains unchanged. Therefore, the brake light may be assumed to be $b_n = 0$. According to model rules (2), (3), some of these steady states are given by inequalities: $t_h < t_s$ and $v_n \leqslant d_n^{\text{eff}}$. Using formulae for the effective distance d_n^{eff} and for times t_h and t_s, the latter inequalities can be written as the conditions for the gap d and the vehicle speed v in the steady states: $d < v \times \min(v, h)$ and $v \leqslant d + \max(\min(d, v) - \text{gap}_{\text{safety}}, 0)$. These conditions together with $v \leqslant v_{\max}$ define the two-dimensional region of the steady states in the speed–gap plane and hence in the flow–density plane (see figure 1, see the appendix for the derivation for the two-dimensional region of the steady states in the speed–gap plane).

In the simulations, the open boundary conditions are applied as follows. We assume that the leftmost cell on the road corresponds to $x = 1$, and the entrance section of the road includes $v_{\max}$ cells. In one time step, when the update of the cars on the road is completed,

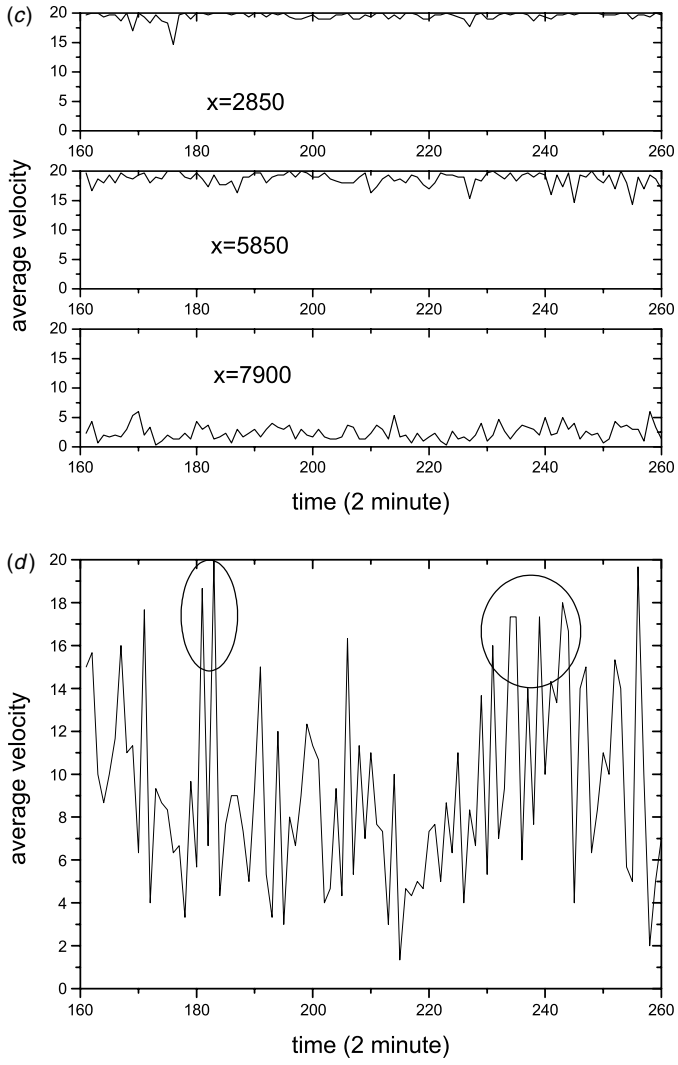

Figure 5. (Continued.)

we check the position of the last car on the road, which is denoted as x_{last}. If $x_{\mathrm{last}} > v_{\max}$, a car with velocity $v_{\max}$ is injected with probability α at the cell $\min[x_{\mathrm{last}} - v_{\max}, v_{\max}]$. On the right boundary, the leading car with the position x_{lead} moves without any hindrance. It is removed if $x_{\mathrm{lead}} > L$ (L denotes the position of the rightmost cell on the road), and the second car becomes the new leading car.

For simplicity, we adopt a simple setup for the on-ramp. At each time step, we scan the positions of the cars and find out the car with number *flag* which is the nearest to the cell $0.8 * L$. Then we check the distance between the car *flag* and its following car $flag - 1$. If $x_{flag} - x_{flag-1} > 10$, then a new car will be inserted into the cells[1] in the middle of the two cars *flag* and $flag - 1$ with probability p_{on}. The velocity of the inserted car equals that of car *flag*, its brake light status is off, its stop time is set to zero.

[1] In the new model, each car has a length of five cells.

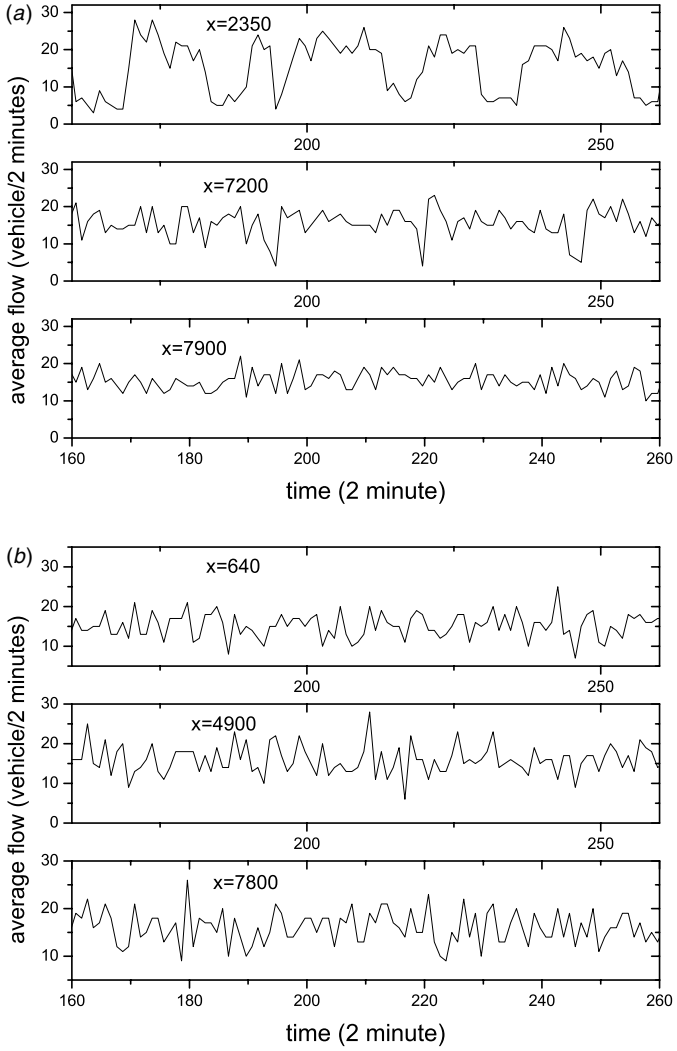

Figure 6. The average flow observed at a fixed location corresponding to figure 5.

In the next section, the simulations are carried out. In the simulations, the parameter values are $t_c = 7$, $v_{\max} = 20$, $p_d = 0.1$, $p_b = 0.94$, $p_0 = 0.7$, $h = 6$, $\text{gap}_{\text{safety}} = 7$. Each cell corresponds to 1.5 m and a vehicle has a length of five cells. One time step corresponds to 2 s.[2] The system size is $L = 10\,000$.

3. Simulation results

In this section, the simulation results are presented. In figure 2, the phase diagram in the (p_{on}, α) plane is shown. It can be seen that the phase diagram is classified into six regions.

[2] This leads to the realistic acceleration value 1.5 m s^{-2}. For such time discretization, the maximum speed corresponds to 15 m s^{-1} (54 km h^{-1}). This corresponds to city traffic. Nevertheless, our further investigation shows that our simulation results are also suitable for freeway traffic ($v_{\max} = 40$).

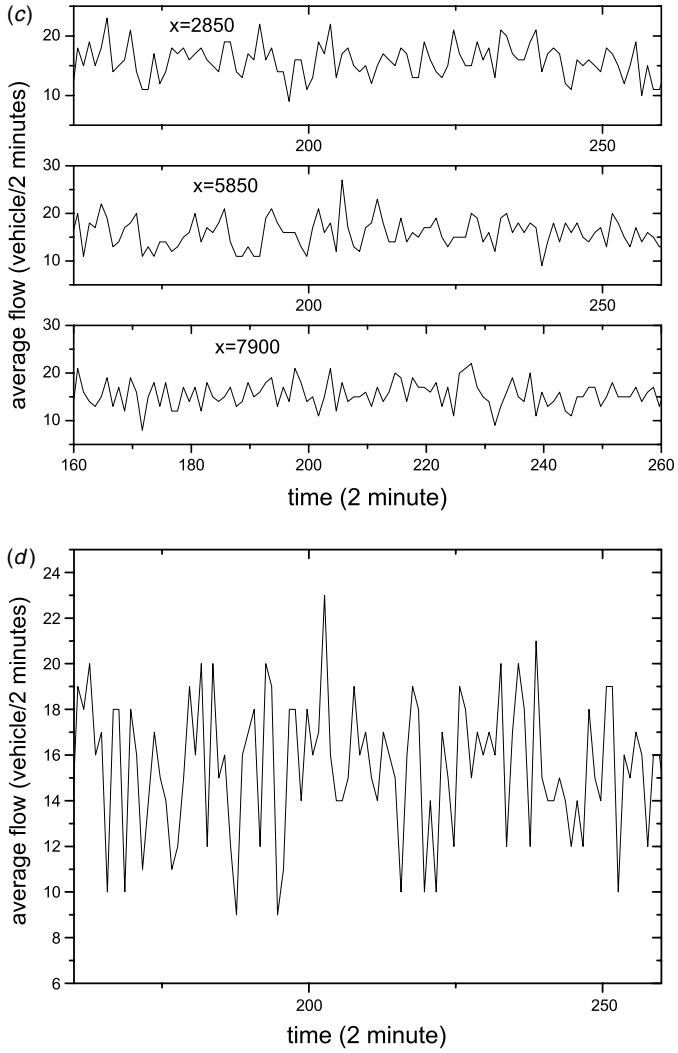

Figure 6. (Continued.)

In region I, a congested pattern occurs where synchronized flow appears upstream of the on-ramp and wide moving jams spontaneously emerge in that synchronized flow. Because this pattern consists of both traffic phases in congested traffic ('synchronized flow' and 'wide moving jam'), it is called 'the general pattern' or 'GP' for short (figures 3(*a*) and (*b*) and figures 4(*a*) and (*b*)) after Kerner.

At high enough values of p_{on} and α, the GP consists of two parts (figures 5(*a*) and 6(*a*)): (a) the spatial–temporal pattern of synchronized flow which is upstream bordered by (b) a sequence of wide moving jams, or the region of wide jams for short. In the flow–density plane, the one-minute averaged data form the jam line 'J' (not shown) for the wide jams region.

This GP resembles the pattern studied in empirical observations [8]. Indeed, as in [8], in the synchronized flow the pinch effect is realized where the vehicle density is high and the

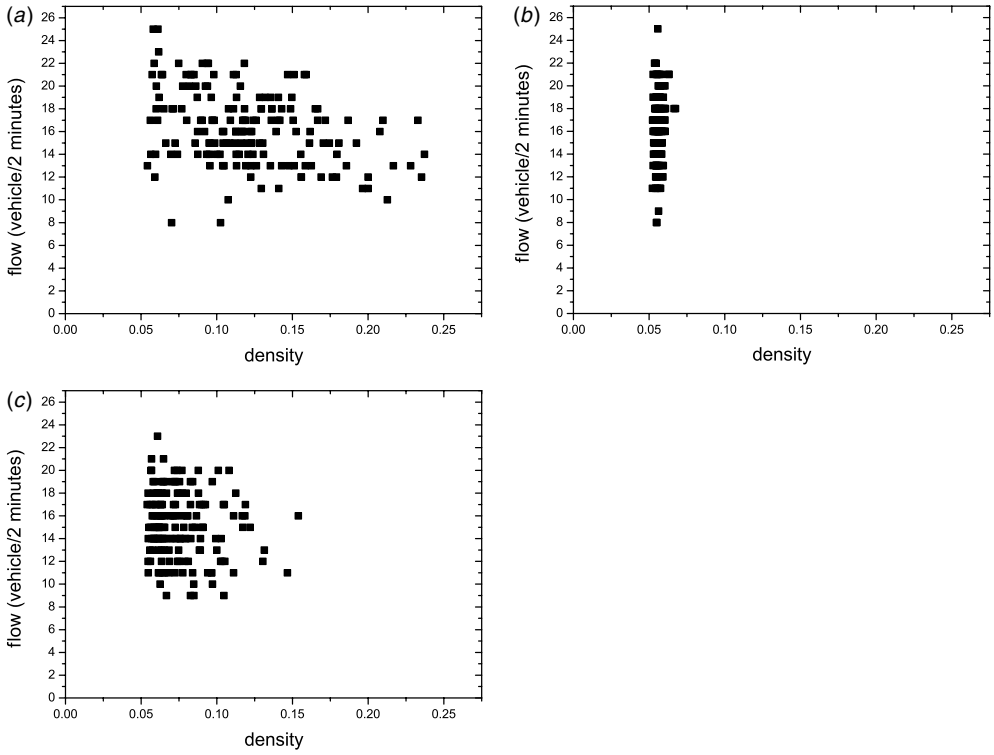

Figure 7. The one-minute averaged data in flow–density plot observed at $x = 7000$. (*a*) Corresponds to figure 3(*c*); (*b*) corresponds to figure 3(*d*); (*c*) corresponds to figure 3(*f*).

vehicle speed is low. In the pinch region, growing narrow moving jams emerge (figures 5(*a*) and 6(*a*), middle). At the upstream boundary (front) of the synchronized flow some of these narrow jams transform into wide moving ones; i.e., the transition from synchronized flow to jam occurs. The successive process of the transformation of narrow moving jams into wide moving jams at the upstream boundary of synchronized flow leads to the formation of the region of wide jams. The upstream boundary of this region is related to the upstream front of the most upstream wide jam. Due to the upstream wide jam propagation, the region of wide jams is continuously widening upstream. But we note that if α is quite large, then the width of the most upstream wide moving jam is a gradually increasing function of time (figures 3(*a*) and 4(*a*)). If in contrast α is small, the most upstream wide moving jam gradually dissolves (figures 3(*b*) and 4(*b*)).

In region II, free flow occurs at the on-ramp (not shown). In regions III, V, congested patterns occur where, in contrast to GP, wide moving jams do not emerge in synchronized flow. These patterns consist of the synchronized flow upstream of the on-ramp only. Therefore such a congested pattern is called 'the synchronized flow pattern' or 'SP' for short (figures 3(*c*)–(*f*) and figures 4(*c*)–(*f*)) after Kerner.

In region III, the downstream front of the synchronized flow is fixed at the on-ramp and the upstream front of it is continuously widening upstream (figures 3(*c*) and 4(*c*)). This widening SP is called 'the widening synchronized flow pattern' or 'WSP' for short after Kerner. In the flow–density plane, the one-minute averaged data are widely scattered (figure 7(*a*)). In

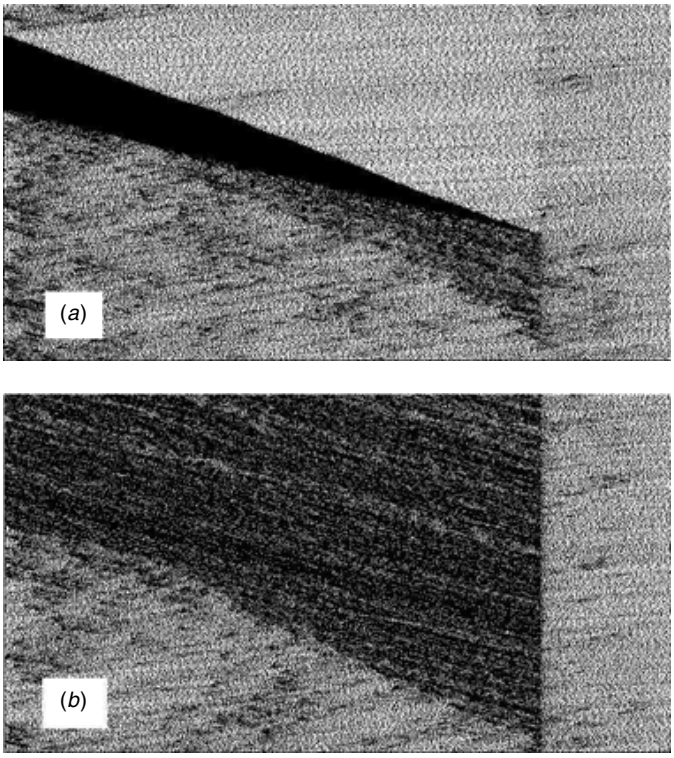

Figure 8. The spacetime plots of the congested patterns. In (*a*), the same parameter values as those in figure 3(*c*) but different random seeds are used; in (*b*), the same parameter values as those in figure 3(*g*) but different random seeds are used. The vertical direction corresponds to 7000 time steps in both (*a*) and (*b*).

region IV, the downstream front of the synchronized flow is still fixed at the on-ramp as in WSP, but the region of the synchronized flow is not continuously widening over time: the region of synchronized flow remains localized at the on-ramp. This localized SP is called 'the localized synchronized flow pattern' or 'LSP' for short (figures 3(*d*) and (*e*) and figures 4(*d*) and (*e*)) after Kerner. In the flow–density plane, the one-minute averaged data are nearly linear outside the LSP region (i.e., in the free flow region, figure 7(*b*)). In both of these synchronized flow patterns (WSP and LSP) the vehicle density is usually lower and the speed is usually higher than the related values inside the pinch region of GP (compare the examples in figures 5(*a*)–(*c*) and figures 6(*a*)–(*c*)). The simulations also show that the width of LSP, i.e., the distance of the upstream LSP front from the on-ramp depends on time and it can show large amplitude complex oscillations (figures 3(*e*) and 4(*e*)). Moreover, the mean width of LSP can depend strongly on q_{on} and α.

In region V, local regions of free flow spatially alternate with local regions of synchronized flow if one observes at a fixed location (figures 3(*f*), 5(*d*) and 6(*d*)). Therefore, it is called 'SP with alternations of free and synchronized flow' or 'ASP' for short after Kerner. In the flow–density plane, the one-minute averaged data are also widely scattered (figure 7(*c*)), but not so widely scattered as in figure 7(*a*).

Finally we study the pattern in region VI. As in GP, a wide moving jam spontaneously emerges in the synchronized flow upstream of the on-ramp. However, since the outflow rate

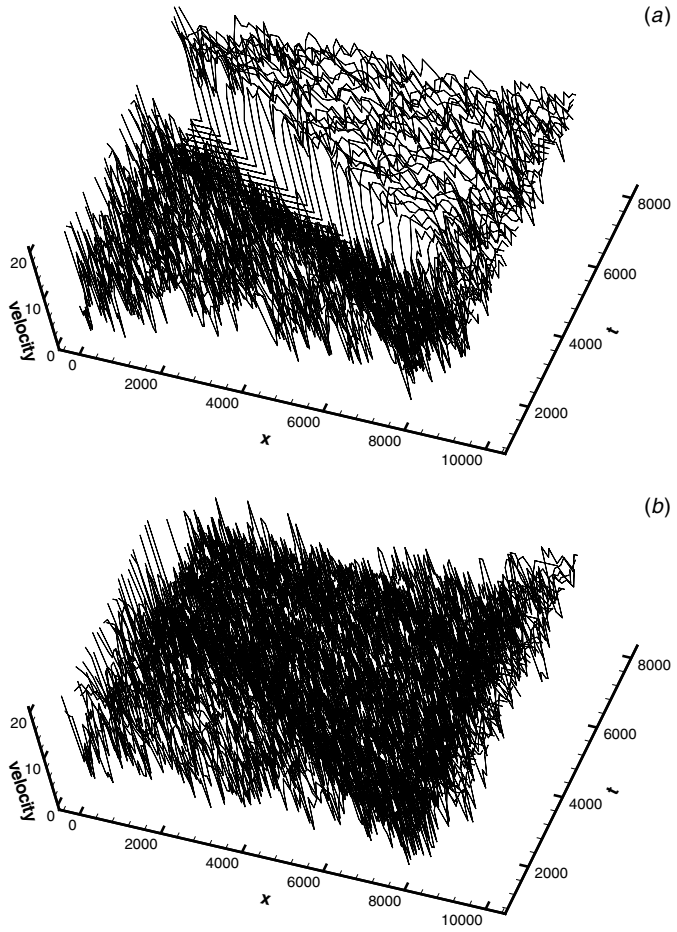

Figure 9. The velocity plots of the congested patterns corresponding to figure 8.

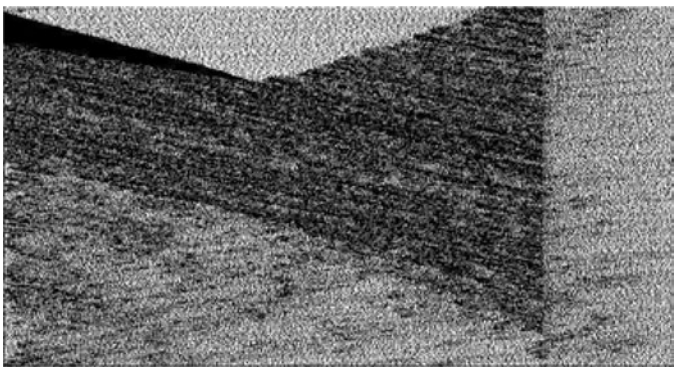

Figure 10. The transformation from WSP to DGP.

of the jam is smaller than the capacity of the on-ramp system, the free flow forms between the location of the on-ramp and the downstream front of the jam (figures 3(g) and 4(g)). Thus, the

pattern is named 'dissolving general pattern' or 'DGP' for short after Kerner. The boundary between regions I and VI intersects the x-axis at the point $P_{\mathrm{on},c}$, at which the capacity of the on-ramp system equals the outflow rate of the jams.

Our simulations also show the metastable effect: in regions III and VI, especially near the boundary between these two regions, either WSP or DGP can occur and exist. In figures 8(a) and 9(a), we show the pattern under the same parameter values as those in figure 3(c) but under different random seeds; one can see that the DGP occurs. Similarly, in figures 8(b) and 9(b), we show the pattern under the same parameter values as those in figure 3(g) but under different random seeds; one can see that WSP occurs. In this sense, region III (VI) is classified based on the criterion that the probability of occurrence of WSP (DGP) is greater than that of DGP (WSP) in the region.

Moreover, the metastable effect can be observed if a large perturbation is exerted. For example, see figure 10. The same parameter values and random seed are used as those in figure 3(c). But when a large perturbation is exerted, e.g., a vehicle stops for 500 s for some reason, the WSP transforms into DGP. However, the DGP cannot transform into WSP.

We compare the results with the empirical observations. It can be found that the phase diagram of the new model is qualitatively similar to the empirical phase diagram (cf figure 26 in [9]): the spatial–temporal features of the congested patterns are consistent with the observations. The difference is that there is no moving SP (MSP) in figure 3. This is due to, in our simulations, the main road being a single-lane road while the observations were carried out on a multi-lane road. This point that no MSP can be observed on a single-lane road is also made by Kerner (see, e.g., [15]).

We also compare the results with those simulated from the cellular automata model [14] and the continuous-in-space microscopic model [13, 16] within the three-phase traffic theory. They are qualitatively the same. The distinction is that ASP is found in our work and in [16] while it is not reproduced in [13, 14].

4. Conclusions

This paper studies the spatial–temporal patterns at an isolated on-ramp using a new cellular automata model based on three-phase traffic theory. The model may describe the synchronized flow, including heavy and light flow, quite satisfactorily [17]. The simulations show that six different regions may be classified in the new model: free flow, GP, WSP, LSP, ASP and DGP. The spacetime plots of the patterns as well as the metastability are investigated. Comparison with the empirical data is made and the qualitative similarity is pointed out.

In this work, the main road is assumed to be single lane. Accordingly, the MSP which is observed on a multi-lane road is not reproduced. In our future work, the extension of the new model to a multi-lane road will be carried out. Moreover, the extension to the congested patterns which occur when two or more bottlenecks exist close to one another is also needed.

Appendix

From $d < v \times \min(v, h)$ and $h = 6$, one has $d < v \times \min(v, 6)$. Therefore, two cases are classified:

$$\text{when} \quad v > 6, \ \text{one has } d < 6v; \tag{1}$$

$$\text{when} \quad v \leqslant 6, \ \text{one has } d < v^2. \tag{2}$$

From $v \leqslant d + \max(\min(d, v) - \mathrm{gap}_{\mathrm{safety}}, 0)$ and $\mathrm{gap}_{\mathrm{safety}} = 7$, one has $v \leqslant d + \max(\min(d, v) - 7, 0)$. Similarly, two cases are classified:

- if $\min(d, v) = v$ (i.e., $d \geqslant v$), then $v \leqslant d + \max(v - 7, 0)$.
  if $v - 7 \geqslant 0$, then $v \leqslant d + v - 7$, one has $d \geqslant 7$. Thus
  $$d \geqslant v \geqslant 7. \tag{3}$$
  if $v - 7 < 0$, then $v \leqslant d$. Thus
  $$d \geqslant v \quad \text{and} \quad v < 7. \tag{4}$$
- if $\min(d, v) = d$ (i.e., $d < v$), then $v \leqslant d + \max(d - 7, 0)$.
  if $d - 7 \geqslant 0$, then $v \leqslant 2d - 7$. Thus
  $$v \leqslant 2d - 7 \quad \text{and} \quad d \geqslant 7 \quad \text{and} \quad d < v \tag{5}$$
  if $d - 7 < 0$, then $v \leqslant d$. This is in contradiction with $d < v$.

Based on equations (1)–(5) together with $v \leqslant v_{\max}$, one derives the two-dimensional region of the steady states in the speed–gap plane and hence in the flow–density plane.

Acknowledgments

The authors are grateful to an anonymous referee for his suggestions to improve the paper. We acknowledge the support from the National Natural Science Foundation in China (NNSFC) with grant no 10272101 and Youth Foundation with grant no KB1330.

References

[1] Schreckenberg M and Wolf D E (ed) 1998 *Traffic and Granular Flow '97* (Singapore: Springer)
Helbing D, Herrmann H J, Schreckenberg M and Wolf D E (ed) 2000 *Traffic and Granular Flow '99* (Berlin: Springer)
[2] Chowdhury D, Santen L and Schadschneider A 2000 *Phys. Rep.* **329** 199
[3] Helbing D 2001 *Rev. Mod. Phys.* **73** 1067
[4] Edie L C 1961 *Oper. Res.* **9** 66
[5] Treiterer J and Myers J A 1974 *Proc. 6th Int. Symp. on Transportation and Traffic Theory* ed D Buckley (London: Reed) p 13
[6] Koshi M, Iwasaki M and Ohkura I 1983 *Proc. 8th Int. Symp. on Transportation and Traffic Flow Theory* (Toronto: University of Toronto) p 403
[7] Kerner B S and Rehborn H 1996 *Phys. Rev.* E **53** R1297
Kerner B S and Rehborn H 1996 *Phys. Rev.* E **53** R4275
Kerner B S and Rehborn H 1997 *Phys. Rev. Lett.* **79** 4030
[8] Kerner B S 1998 *Phys. Rev. Lett.* **81** 3797
[9] Kerner B S 2002 *Phys. Rev.* E **65** 046138
[10] Berg P and Woods A 2001 *Phys. Rev.* E **64** 035602
[11] Helbing D, Hennecke A and Treiber M 1999 *Phys. Rev. Lett.* **82** 4360
Treiber M, Hennecke A and Helbing D 2000 *Phys. Rev.* E **62** 1805
[12] Lee H Y, Lee H W and Kim D 1998 *Phys. Rev. Lett.* **81** 1130
Lee H Y, Lee H W and Kim D 1999 *Phys. Rev.* E **59** 5101
[13] Kerner B S and Klenov S L 2002 *J. Phys. A: Math. Gen.* **35** L31
[14] Kerner B S, Klenov S L and Wolf D E 2002 *J. Phys. A: Math. Gen.* **35** 9971
[15] Kerner B S 2001 *Preprint* cond-mat/0211684
[16] Kerner B S and Klenov S L 2003 *Phys. Rev.* E **68** 036130
[17] Jiang R and Wu Q S 2003 *J. Phys. A: Math. Gen.* **36** 381
[18] Knospe W, Santen L, Schadschneider A and Schreckenberg M 2000 *J. Phys. A: Math. Gen.* **33** L477